FINITE ELEMENT SIMULATION OF MACROSCOPIC MACHINING PROCESSES - IMPLEMENTATION OF TIME DEPENDENT DOMAIN AND BOUNDARY CONDITIONS

C. NIEBUHR, D. NIEDERWESTBERG, AND A. SCHMIDT

Abstract. In this article, the modeling and simulation of material removal during machining processes with a finite element method is discussed. The model links a dexel based material removal simulation with a thermomechanical finite element method to forecast thermical and process-related shape errors during machining processes. It is modeled mathematically by linking heat conduction equation with the deformation equation on a time dependent domain including moving boundaries. We present here details from the finite element implementation. The project is financed by DFG via SPP1480.

1. Introduction

The minimization of shape errors during dry machining processes like milling and drilling processes is a major challenge to modern production cycles. Considering these thermomechanical effects in the NC-simulation offers great advantages for reduction of shape errors during machining processes. To achieve this goal a new method of material removal simulation in due consideration of thermomechanical effects is presented. While thermomechanical effects are modeled by a finite element (FE) simulation, the material removal is done by a dexel model. In combination with a process model for prediction of cutting forces and heat flux, thermal and mechanical effects during the process are reproduced realistically on the workpiece. This creates a closed simulation system that considers thermomechanical interdependencies. We consider here a macroscopic model which includes the microscopic effects of chip formation and removal only via the process model, [7, 8].

The so called dexel ("depth pixel" or "depth picture element") model is comparable to a plain grid of parallel nails of different length. Earlier approaches used elements of only one direction, like for example the graphics rendering in graphics processor units (z-buffer), [15]. To decrease the dependency between the chosen dexel direction, the shape of the workpiece and the resulting accuracy, multi-dexel models have been introduced [4, 9, 12]. Usually three grids are used oriented to the main axes of a cartesian coordinate system.

An approach for modeling heat conduction and thermomechanical workpiece characteristics is the finite element (FE) model. It was used in several investigations for modeling of machining processes [5, 10]. Especially the mapping of heat fluxes und process forces during continious (milling) and discontinious (drilling) processes to boundary conditions on a moving boundary is a challenge. Analytical and numerical studies of the propagation of discretization errors in adaptive methods for related problems are presented in [1–3].

The NC-Simulation has to be extended with several properties to emulate thermomechanical effects. These extensions can be divided analytically into two components, the process model and the workpiece model.The workpiece model describes the actual state of the workpiece in geometrical and thermomechanical aspects

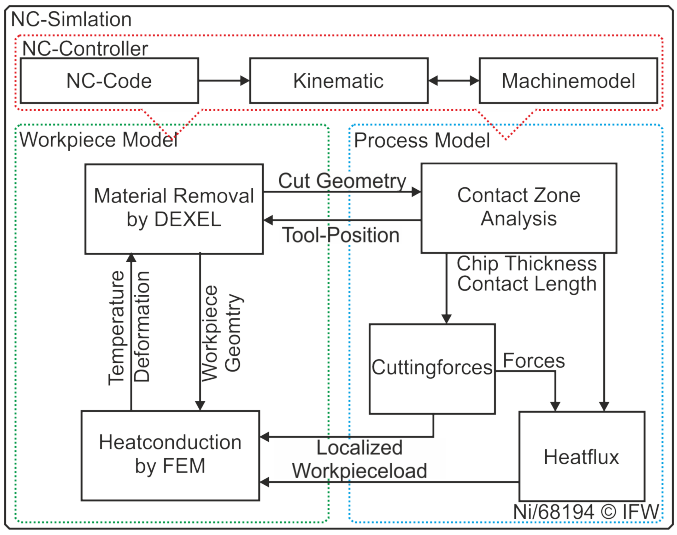

FIGURE 1.1. Detailed simulation cyrcle of data flow.

(Fig. 1.1 left). Additional material removal algorithms allow changing the geometrical representation of the workpiece, while thermal conduction algorithms allocate modify the thermal condition of the workpiece.

The material removal process is controlled by a classical NC-Simulation, with kinematics and NC-Controller (Fig. 1.1 top) [6], for a realistic thermomechanical simulation the boundary conditions of the workpiece have to be changed by a process model. This process model has several sequences (Fig. 1.1 right). The local cutting conditions are calculated from the material removal process. With this data a cutting force and heat flux prediction is triggered that calculates the mechanical and thermal load. This changes the boundary conditions of the workpiece model, especially in the FE simulation.

The major aspect of this paper is the modeling of the workpiece model in his mathematical representation in the FE model with its input and output parameters (Fig. 1.1 left). The contact zone analysis and cutting force had been shown in [14]. Linking the FE model for the heat conduction analysis and deformation behaviour to a dexel model for the material removal process allows considering both, volumetric changes and thermomechanical deformation, in the NC-Simulation, [8]. Thereby these components are considering the information of each other, so that the resulting effects can be modeled. Here, the volume changes described by the material removal process is taken into account in the FE simulation for a more realistic heat conduction and workpiece deformation simulation. As input parameters for the FE simulation, moving heat sources and process forces has to be extracted from the material removal process and could only consider over the boundary conditions in the FE model. Moreover the surface of the workpiece and the boundary conditions of the process model changed in the dexel model by the current mechanical deformations and temperature distributions determinded by the FE simulation.

For the linking of all components a XML based communication system was implemented that is characterized by high flexibility and fault tolerance as shown in [13]. Thereby the pure thermoelastical simulation and the NC-Simulation run and communicate in synchronized unequal time steps.

2. Mathematical model

The model of thermomechanical effects during machining processes includes the classical formulations of the heat equation and the quasi-stationary deformation equation on time dependent domains with moving boundary conditions.

We assume that the time dependent domain is a subset of a fixed $\Omega \subset \mathbb{R}^d$ with $d = 3$. A corresponding model could also be applied in dimensions $d < 3$.

2.1. **Heat equation.** Let $\Omega = \Omega_s(t) \cup \Omega_m(t) \cup \Gamma_N(t) \subset \mathbb{R}^d$ be the time dependent partition of the domain Ω for $t \in [t_0, t_1]$, consisting of a solid subdomain $\Omega_s(t)$ and a removed subdomain $\Omega_m(t)$ with $\Omega_s \cap \Omega_m = \emptyset$. The domain boundary $\partial\Omega_s(t)$ is subdivided in parts with different boundary conditions, $\Gamma_N(t)$ and $\Gamma_R(t)$. Here, $\Gamma_N(t)$ denotes the moving boundary between the solid and the removed subdomain. A sketch of the different domains and their boundaries is given in Figure 2.1. Initially, we start with $\Omega_m(0) = \emptyset$, $\Gamma_N(0) = \emptyset$ and $\partial\Omega_s(0) = \Gamma_R(0) = \partial\Omega$.

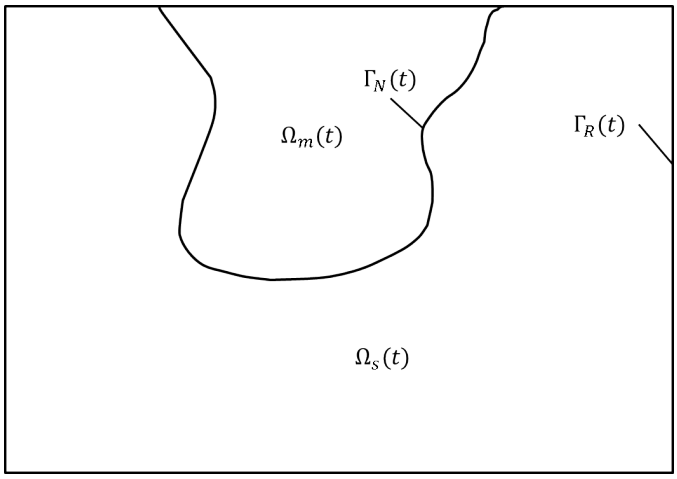

Figure 2.1. 2D sketch of a time-dependent moving boundary problem on domain $\Omega = \Omega_s(t) \cup \Omega_m(t)$.

The process is modeled by the heat equation only on $\Omega_s(t)$ for the temperature $\theta : \Omega_s(t) \to \mathbb{R}^d$ with temperature dependent material properties of the density $\rho(\theta)$, the specific heat capacity $c_e(\theta)$ and the heat conductivity $\kappa(\theta)$.

The heat equation is given by the PDE-System

$$\rho c_e \frac{\partial}{\partial t}\theta - \text{ div } (\kappa \nabla \theta) = 0 \qquad \text{in } \Omega_s(t), \tag{2.1}$$

where we assume the absence of interior heat sources. To complete the problem, we add conditions on the boundary. To model thermal radiation and convection cooling, we choose a Robin boundary condition on $\Gamma_R(t)$. In this case the heat flux over the boundary is proportional to the temperature between the interior and the external temperature θ_{ext}. We obtain the following equation, where α is the heat transfer coefficient and $\mathbf{n}$ the outer normal vector.

$$-\kappa \nabla \theta \cdot \mathbf{n} = \alpha(\theta - \theta_{ext}) \qquad \text{on } \Gamma_R(t). \tag{2.2}$$

A Neumann boundary condition $\Gamma_N(t)$ is used for the moving boundary part. In this case the heat flux over the boundary would be described by a time and space dependent function $g_1(x, t)$ for the incomming flux generated by the machining

process.

$$-\kappa\nabla\theta\cdot\mathbf{n} = g_1(x,t) \qquad \text{on } \Gamma_N(t). \tag{2.3}$$

In this way, equations (2.1), (2.2) and (2.3) give us the complete inital boundary value problem for heat conduction on time dependent domains.

2.2. **Deformation behaviour.** In this section we introduce the model for deformation behaviour. We consider infinitesimal strain which means that the occurring deformations are "small". The assumption of small strains is valid for the settings of heat treatment with moderate external forces, we are dealing with. We introduce the balance of momentum which is fundamental in continuum mechanics.

Let $\Omega_s(t)$ be the reference configuration for $t \in [t_0, t_1]$. The displacement vector is defined as $\mathbf{u} : \bar{\Omega}_s(t) \to \mathbb{R}^d$. We consider here a linear elasticity model for an isotropic material, where the stress tensor $\sigma(u) \in \mathbb{R}^{d\times d}$ is given by

$$\sigma(\mathbf{u}) = \lambda tr(\epsilon(\mathbf{u}))\mathbf{I} + 2\mu\epsilon(\mathbf{u}) \tag{2.4}$$

with Lamé coefficients λ, μ and the linearized strain tensor

$$\epsilon(\mathbf{u}) := \frac{1}{2}\left(\nabla\mathbf{u} + (\nabla\mathbf{u})^T\right). \tag{2.5}$$

As the time scale for heat conduction is much slower than that for mechanical wave equation, we use here the elliptic quasi-stationary deformation equation on the time dependent domain with forces $\mathbf{f}$ from thermal expansion and maybe gravitation on the right hand side,

$$-\text{ div }(\sigma(\mathbf{u})) = \mathbf{f} \qquad \text{in } \Omega_s(t), \tag{2.6a}$$

$$\mathbf{u} = \mathbf{g}_{fix} \qquad \text{on } \Gamma_{fix}(t), \tag{2.6b}$$

$$-\sigma(\mathbf{u})\cdot\mathbf{n} = \mathbf{g}_2(x,t) \qquad \text{on } \Gamma_{free}(t) \tag{2.6c}$$

or, expressing the stress tensor via the strain tensor,

$$-\mu\Delta\mathbf{u} - (\mu+\lambda)\text{ grad div }\mathbf{u} = \mathbf{f} \qquad \text{in } \Omega_s(t), \tag{2.7a}$$

$$\mathbf{u} = \mathbf{g}_{fix} \qquad \text{on } \Gamma_{fix}(t), \tag{2.7b}$$

$$-\left(\lambda(tr(\epsilon(\mathbf{u})))\mathbf{I} + 2\mu\epsilon(\mathbf{u})\right)\cdot\mathbf{n} = \mathbf{g}_2(x,t) \qquad \text{on } \Gamma_{free}(t). \tag{2.7c}$$

Here we chose Dirichlet boundary conditions to prescribe the displacement $\mathbf{g}_{fix}$ on a boundary part $\Gamma_{fix}(t)$ and Neumann boundary condition to apply external forces via a time and space dependent function $\mathbf{g}_2(x,t)$ on $\Gamma_{free}(t)$, where the domain boundary is devided into

$$\partial\Omega_s(t) = \Gamma_{fix}(t) \cup \Gamma_{free}(t).$$

2.3. **Coupled Problem.** In this section we want to present the fully coupled thermomechanical problem. So mainly we gather the above presented equations but we also introduce the coupling therms. We present the equations with emphasis on the dependencies between the different quantities.

Due to the slow time scale of heat conduction, we ignore effects of dissipation. Thus, only the mechanical effect of domain deformation enters the heat equation. For small deformations, this is typically ignored.

The coupling between temperature and deformation is due to thermoelasticity. The Lamé coefficients can be considered to be temperature dependent, and the stress tensor is augmented by a term for thermal expansion reflecting density changes due to heating and cooling,

$$\sigma(\mathbf{u}) = 2\mu(\theta)(\epsilon(\mathbf{u}) + (\lambda(\theta)tr(\epsilon(\mathbf{u})) - 3\alpha(\theta-\theta_0))\,\mathbf{I}, \tag{2.8}$$

with the thermal expansion coefficient α and initial temperature θ_0.

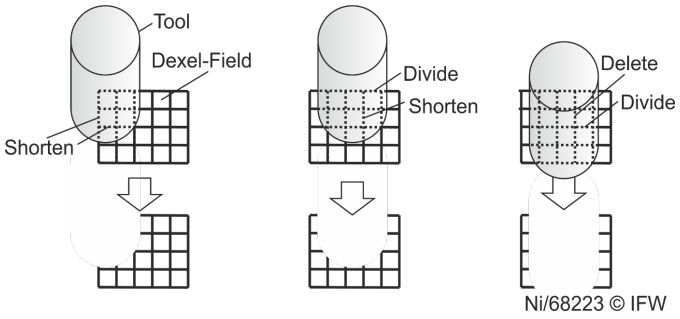

FIGURE 3.1. 2D-Boolean-Dexel-Operations

3. Thermomechanical Dexel model

The simulation of material removal processes can be done by the so called dexel ("depth pixel" or "depth picture element") model [4, 9, 12, 15]. For the modelling of the material removal process during the simulation of cutting processes, three Boolean-Operations are used, see (Fig. 3.1). Due to the method of machining the most used operation is shorten, where the dexel-end- or startpoint is shifted. In the case of undercut operations the dexel is divided. If a dexel has to be divided an additional dexel has to be included in the raster of the model on same position and both dexel are shortened. The last Boolean-Operation is the deletion, which has to be called when all material in one field of the model is machined. In this case the dexel is set to an invalid status and no start- or endpoint exist.

To consider the thermomechanical effects in the material removal simulation, the dexel model has to be extended by thermomechanical information. Temperature and deformation of the workpiece are specific data that have to be known and transfered into the dexel model.

The data structure of the dexel model enables a geometric representation of the workpiece surface by discrete start and endpoints of the dexels (Fig. 3.3). In cutting operations only near-surface areas are machined. Caused by this fact, only information in these areas of the workpiece is relevant for the material removal simulation. Therefore, an extension of the existing structure is only necessary in the start and endpoints of the dexels. To consider temperature and deformation, a dexel point was extended by a temperature value and a deformation vector. Using a deformation vector instead of alternative methods, like shortening and lengthening of the dexel or shifting of dexel points, gives essential advances. These are:

- keeping the consistency of the workpiece model,
- easier linking to the FE model structure,
- parallel representation of the chilled workpiece by the basic dexel structure.

Current thermomechanical data, continuously imported from the FE model into the dexel structure, now allows considering the thermomechanical effects in the NC-Simulation. These effects are caused by the local temperature and the local deformation of the workpiece in the cutting zone, see Fig. 3.2.

The actual temperature of the workpiece has a major influence on the specific characteristics of the material like shear yield stress and therefore on the resulting cutting forces.

The deformation of the workpiece globally influences the dimension of depth a_p and width a_e of cut and the geometric representation of the workpiece. Therefore, the deformation determined by analyzing the sweep-surface DCPs is inversely projected onto the cutting tool (Fig. 3.3). By this method, the thermomechanical

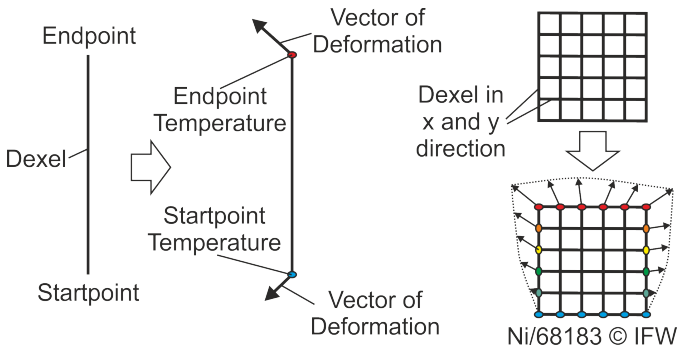

FIGURE 3.2. Thermomeachanical extended Dexel-Structure

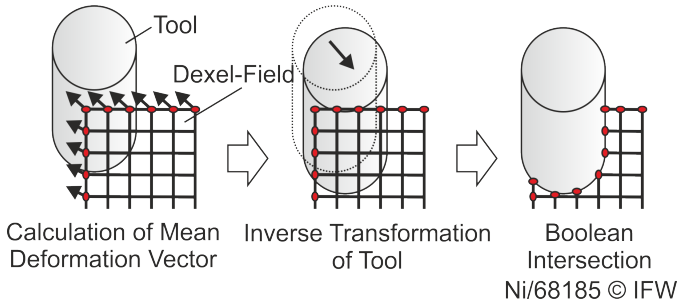

FIGURE 3.3. Considering thermomechanical Deformation

deformation of the workpiece can be considered and the resulting shape errors can be predicted.

4. NUMERICAL APPROACH

Numerical implementations of the thermoelastic model and the linking to the dexel model have been integrated via the finite element toolbox ALBERTA. How to handle the communication between the two models, to simulate the material removal, and to implement the boundary conditions for the PDE system is shown in this section.

4.1. **ALBERTA.** To compute heat conduction as well as thermomechanical elastic (and maybe plastic) deformation of the workpiece, the equations are discretized and simulated by a FE simulation. We are using a FE model that is based on the adaptive finite element toolbox ALBERTA, [11]. This Toolbox is using unstructured simplicial meshes, like tetrahedrons in 3D, together with local adaptive mesh refinement and coarsening for appropriate approximation of domain and solutions, which is crucial for the simulation of machining processes.

4.2. **Communication between FE and Dexel model.** To consider the material removal of the dexel model also in the FE simulation, the two models are linked. This linking of the models is based on the interchange of parameters and values such as the geometry of the workpiece, the thermomechanical displacements of the workpiece as well as heat flux and process forces produced by the cutting process.

To realize the interchange of information between the two models, an XML based communication system was implemented, which is used at a given timestep, [13]. In this system the geometrical information of the workpiece surface and other

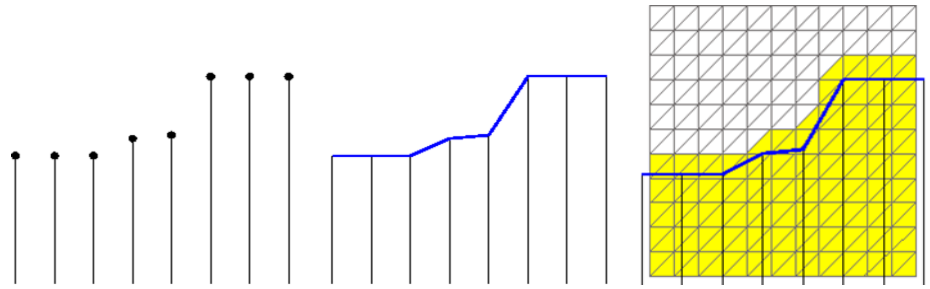

(a) Dexel representation in one direction (b) Interpolation of domain boundary with graph G (c) Dexel – FE-mesh overlay

FIGURE 4.1. Sketch of virtual-domain approach

information given at the dexel points described by the dexel fields in different directions (x-, y- and z-direction) is provided to the FE model. The FE model uses the information of the workpiece surface to determine $\Omega_s(t)$. Then the information of heat fluxes and process forces are projected on the boundary surface of $\partial\Omega_s(t)$ (see Section 4.4) and the linear systems of heat conduction and deformation are solved. At last the numerical results of temperature and deformation are given back to the dexel model via the communication system. This enables the use of thermomechanical information in the material removal and process models.

A more detailed description, how to include geometrical data as well as local heat fluxes and process forces into the FE model is given in the next sections.

4.3. **Discretization of material removal in finite element method.** The material removal simulation and thus time dependent domain is realized in the FE model by using a time dependent subdomain $\Omega_s(t)$, which was considered first in Section 2.1.

Another approach to handle a time dependent domain might be a moving mesh approach, where the nodes are moved in every timestep in order to represent the current geometry. Due to large deformations by material removal, a frequent remeshing would be necessary in order to prevent distorted elements. Thus, the moving mesh approach is not used here.

We use a discrete approach on a fixed domain $\Omega = \Omega_{s,h}(t) \cup \Omega_{m,h}(t)$ with an admissible triangulation

$$\Omega = \bigcup_{S \in \mathcal{S}} S \subset \mathbb{R}^d.$$

The mesh represents the full initial workpiece from which the finished workpiece is made. To implement material removal, appropriate simplizes S are 'removed' respectively blinded out.

Determined by the current coordinates of the dexel endpoints from the dexel model (Fig. 4.1(a)), an interpolated piecewise bilinear surface G defines the current boundary surface of the time dependent domain, see Fig. 4.1(b). For each element of the triangulation, it is then easy to decide whether the element is fully outside of the current domain or not, Fig. 4.1(c). Such fully outside elements will not be considered anymore in the calculation and will thus be ignored during all following time steps of the simulation. The algorithm to set the discrete subdomain $\Omega_{s,h}(t)$ respectively the removed subdomain $\Omega_{m,h}(t)$ is as follows:

4.1. **Algorithm** (Set subdomain)**.**

`subroutine set_subdomain(`$\mathcal{S}$`)`

$\Omega_{s,h}(t) = \Omega_{m,h}(t) = \emptyset$

```
for all S ∈ 𝒮 do
  get world coordinates of vertices n
  for all n ∈ S do
    loop over all dexelfields
      find supporting points for n in the dexelfield
      interpolate graph G over supporting points
        if n below interpolated graph G
          mark n as in_subdomain
        else
          mark n as outside
        end if
    end loop
  end for
  if one or more vertices n marked as in_subdomain
    Ω_{s,h}(t) = Ω_{s,h}(t) ∪ S
  else
    Ω_{m,h}(t) = Ω_{m,h}(t) ∪ S
  end if
end do
```

To get a sufficiently good approximation of the current workpiece, a specific algorithm for control of the adaptive local mesh refinement is implemented. In order to have an accurate approximation of the workpiece surface with simplizes S, appropriate local refinement and coarsening operations are used. First, we introduce a specific refinement marking strategy in the local region near the moving workpiece surface $\Gamma_{N,h}(t)$.

4.2. **Algorithm** (Marking simplex near the workpiece boundary for refinement)**.**

```
subroutine refine_subdomain(𝒮)
  do for S ∈ 𝒮
    get world coordinates of vertices n
    for all n ∈ S do
      loop over all dexelfields
        find supporting points in the dexelfield
        interpolate graph G over supporting points
        if graph G intersects simplex S and refine_level < limit
          mark S for refinement
        end if
      end loop
    end for
  end do
  refine_mesh(𝒮)
```

Here, we use again the bilinear interpolation of the dexel endpoint coordinates over each dexel field to define the surface graph G. Then we check whether G intersects the simplex S and whether the refinement level of this simplex is smaller than a given limit, which might be chosen before the simulation starts, or computed from approximation estimates for $\Gamma_N(t)$.

The algorithm of coarsening the mesh is a bit more involved. Here we have to check whether the simplex is located in the interior of $\Omega_{s,h}(t)$, $\Omega_{m,h}(t)$ or in the border zone between the two domains. While the simplizes in $\Omega_{m,h}(t)$ might be coarsened without difficulties, the simplizes in $\Omega_{s,h}(t)$ can only be coarsend with the standard adaptive strategies for FEM. In order to prevent a too coarse mesh in

the border zone of the two domains, the coarsening is limited here. The algorithm for one simplex is as follows.

4.3. **Algorithm** (Marking one simplex for coarsening)**.**

```
subroutine coarse_mark_fct(S, 𝒮)
  do for S ∈ 𝒮
    if S → in_subdomain = 0
      mark = number of neighbor elements in subdomain
      if mark = 0
        mark S for coarsen
      end if
    else if S → in_subdomain = 1
      mark = number of neighbor elements in subdomain
      if mark = number of neighbours
        use FEM coarsen strategie
      end if
    else
      if (refine_level > limit)
        mark S for coarsen
      else
        do nothing
      end if
    end if
  end do
  coarse_mesh(𝒮)
```

In this way, the heat and deformation equations are solved only on a subset $\Omega_{s,h}(t)$ of the complete domain Ω as described in Section 2. With the given local adaptive refinement and coarsening algorithms, the time dependent domain and moving boundary can be approximated by the mesh as accurately as desired.

4.4. **Boundary data for the FE model.** Boundary conditions are given by the process model, which is included in the dexel model. Neumann and / or Robin conditions, like heat flux and process forces, have now to be given on the boundary of the subdomain $\Omega_{s,h}(t)$, which is at least partly composed of interior sides of elements of the original triangulation of Ω. We explain here in more detail, how to apply the boundary data on the discrete boundary $\partial\Omega_{s,h}(t)$ in the FE simulation.

As known from Section 4.2, boundary data is given by the process model included in the dexel model. In the FE simulation, such data is included via the boundary conditions in heat conduction and deformation equations. During the approximation of the current workpiece surface $\partial\Omega_s(t)$ with the refinement and coarsening algorithms described above, we typically get for the discretized $\partial\Omega_{s,h}(t)$ a larger surface area, than for the relativly smooth surface given by the geometrical information from the dexel model. Locally, we may get a much larger surface area (a factor around $\sqrt{2}$ in 2D), see Figure 4.2(a).

Thus, a simple transfer of the boundary data $g_1, \mathbf{g}_2$ for heat flux and process force would induce an excessive warming respectively force effect. An adaption to the boundary discretization is necessary. A suitable scaling factor is given by the scalar product of the two normal vectors of the discretized and the continuous boundary which is the cosine of the enclosed angle α. This is given by

$$\cos\alpha(\mathbf{n}_\Gamma, \mathbf{n}_{\Gamma_h}) = \frac{\mathbf{n}_\Gamma \cdot \mathbf{n}_{\Gamma_h}}{||\mathbf{n}_\Gamma|| \cdot ||\mathbf{n}_{\Gamma_h}||} \tag{4.1}$$

In order to prevent that one of the computed normal vectors does not have the length 1, we use the above normalized representation.

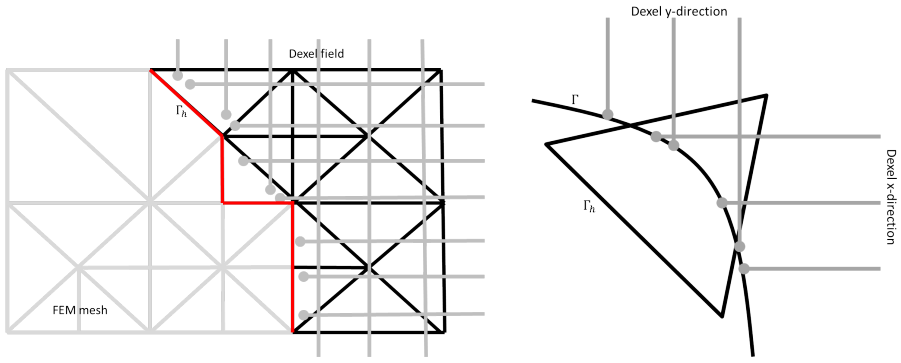

(a) Dexel field and FEM mesh overlay (b) Zoomed sketch for one simplex

FIGURE 4.2. Sketch of boundary attachment at the moving boundary part

Through the different discretizations in FE and dexel models, only information on a few dexel points could be assigned on the boundary of a simplex S. To compensate for that, supporting points over all dexel fields are used for each quadrature point x of the suface of simplex S. These supporting points are used again for a bilinear interpolation of data. For the ith supporting point, $i = 1, .., 4$, we use heat flux data

$$\tilde{q}_i = q_i \cdot \cos\alpha(\mathbf{n}_h, \mathbf{n}_i)$$

with heat flux q_i given from the process model and normal vectors $\mathbf{n}_i$ of the continuous surface $\Gamma_N(t)$ and $\mathbf{n}_h$ of discrete boundary $\Gamma_{N,h}(t)$. With bilinear interpolation over each dexel field with interpolation operator I_h, we get finally for the discrete formulation of the Neumann boundary condition (2.3) the following data at a quadrature point x,

$$g_{1,h}(x,t) = \frac{1}{d}\sum_{k=1}^{d} I_h\left(x, \tilde{q}_1^k, \tilde{q}_2^k, \tilde{q}_3^k, \tilde{q}_4^k\right) \tag{4.2}$$

where d is the number of given dexel fields.

Analogous to this, we derive data $\mathbf{g}_{2,h}$ for the weak formulation of the Neumann boundary condition of deformation equation (2.7c). For each supporting point we get

$$\tilde{\mathbf{f}}_i = \mathbf{f}_i \cdot \cos\alpha(\mathbf{n}_h, \mathbf{n}_i)$$

with force vector $\mathbf{f}_i$ and normal vectors as above. By interpolation, this gives for each quadrature point x on $\Gamma_{free,h}(t)$

$$\mathbf{g}_{2,h}(x,t) = \frac{1}{d}\sum_{k=1}^{d} I_h\left(x, \tilde{\mathbf{f}}_1^k, \tilde{\mathbf{f}}_2^k, \tilde{\mathbf{f}}_3^k, \tilde{\mathbf{f}}_4^k\right). \tag{4.3}$$

Using these modifications of the boundary data from the dexel model, we get a good approximation of the total fluxes and forces in the FE model.

5. RESULTS

We describe here the algorithm of our coupled dexel – finite element approach and present results from the simulation of a milling process.

The algorithm for the simulation is based on the interaction between the two models. After initialization of both models, communication is performed in each time step, see Algorithm (5.1).

First, the mapping of the current workpiece surface and the attached boundary data is transfered from the dexel model to the FE model. After solving the heat conduction and deformation equations based on these boundary data, the temperature und deformation values at the dexel endpoints are computed. This information is transfered back to the dexel model. In the dexel model, the deformation is used in the next material removal simulation, and temperature values enter the process model for computation of forces and heat sources generated by the local machining process. This is repeated for each time step until the final time t_{end} of the simulation is reached.

5.1. **Algorithm** (Coupling of dexel and finite element simulation)**.**

```
initialization of dexel and FE model
do for each timestep
   · data exchange from dexel to FE model
   · in FE model
      · mapping the workpiece surface
      · attache boundary information
      · solve heat equation
      · solve deformation equation
   · data exchange from FE to dexel model
   · in dexel model
      · mapping deformation information in the dexelfields
      · do material removal simulation
      · compute process forces
      · compute heat fluxes
end do
```

We present now results from the thermomechanical simulation of a milling process, which was also done and measured experimentally.

The material of this workpiece is C45EN, original size is $40 \times 195 \times 40mm^3$. In the process, a cavity is milled out of the cuboid, leaving a bar of $2mm$ thickness. The whole process included 26 rough and 7 fine machining steps.

Measurements included temperature as well as supporting and process forces. For measuring temperature, five thermoelements of type K (NiCr-Ni) with measurement amplifier SAK12-461-100-10 were inserted at different positions, see Figure 5.1(c). For measuring forces, the workpiece was fixed between two dynamometers to get the workpiece statically determined. The supporting and process forces were measured by eddy current sensors from Kistler type 9257B and amplifier 5070A. The production of the component was done on a HELLER MCi16.

The Figures 5.1(a)-(d) show the subdomain approximation of material removal and temperature distribution on the surface at different times during roughing. A snap-shot of temperature distribution during finishing is given by Figure 5.1(e) and the final (nearly room) temperature distribution at the workpiece surface after finishing is given in Figure 5.1(f). The figures show clearly that the heat enters in the current milling zone producing large temperature gradients, while the conduction of heat into the workpiece goes slowly.

Figure 5.2 depicts the temperature profiles at the five measuring points in experiment (Fig. 5.2(a)) and simulation (Fig. 5.2(b)). The profiles are quite similar to each other, but show some mismatches in the peaks, expecially for the finishing step. These discrepancies may result from imprecise boundary data and/or discretization issues and will be adressed in near future.

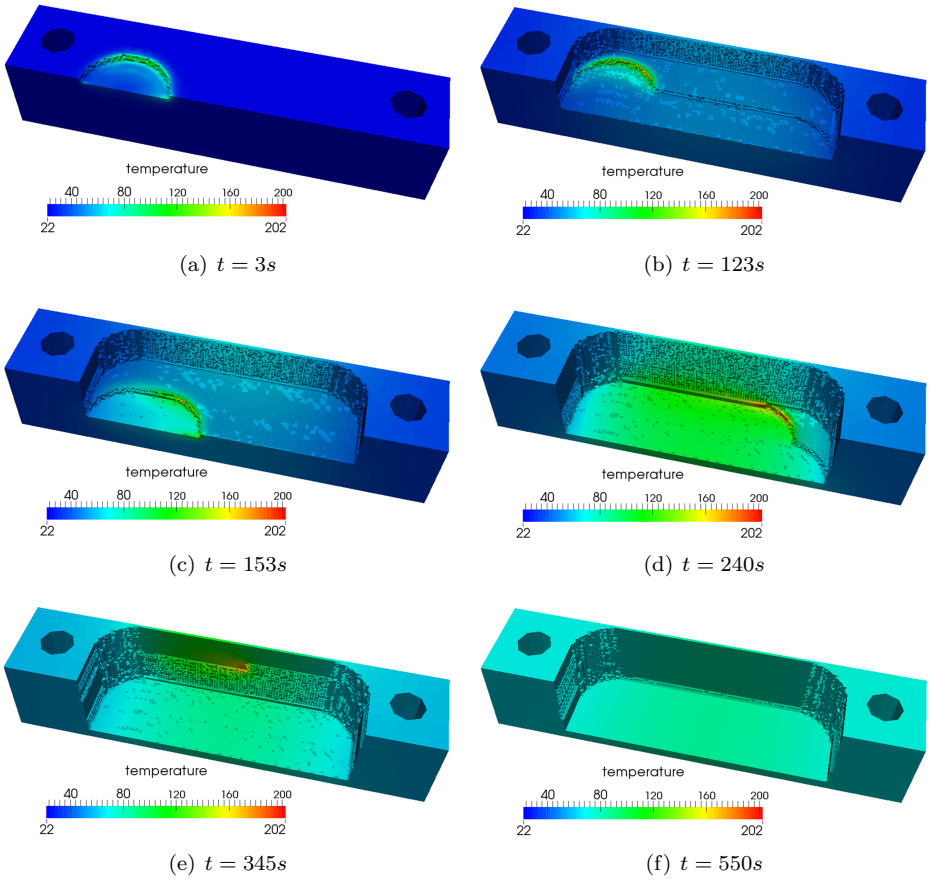

(a) $t = 3s$ (b) $t = 123s$

(c) $t = 153s$ (d) $t = 240s$

(e) $t = 345s$ (f) $t = 550s$

FIGURE 5.1. Simulation of milling process: workpiece with surface temperature at different times

6. SUMMARY

A simulation model for the identification of dimension and shape errors in machining processes caused by thermomechanical effects has been derived by linking a thermomechanic finite element method with a dexel based material removal simulation. The coupled model already shows quite good correspondance between results from simulation and experiments.

Based on this model, we plan to develop a compensation strategy for thermomechanically induced manufacturing imprecisions by adjusting in advance the process parameters and machining tool path plan.

ACKNOWLEDGEMENT

The authors gratefully acknowledge the financial support by the DFG (German Research Foundation) for the research project "Thermomechanical Deformation of Complex Workpieces in Drilling and Milling Processes" (DE447/90-2, MA1657/21-2) within the DFG Priority Program 1480 "Modeling, Simulation and Compensation of Thermal Effects for Complex Machining Processes".

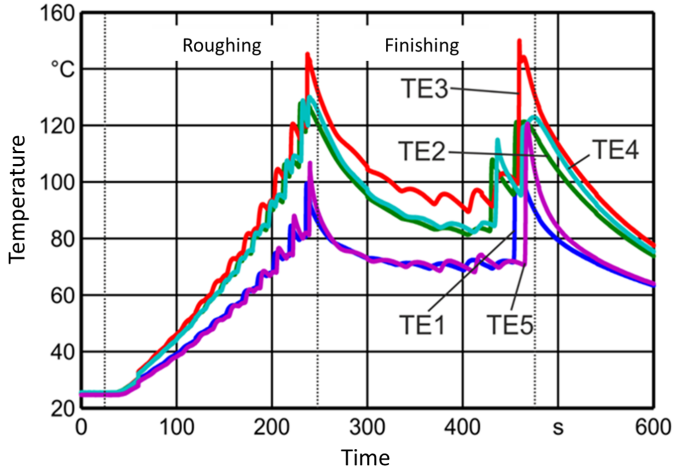

(a) Temperature in experiment

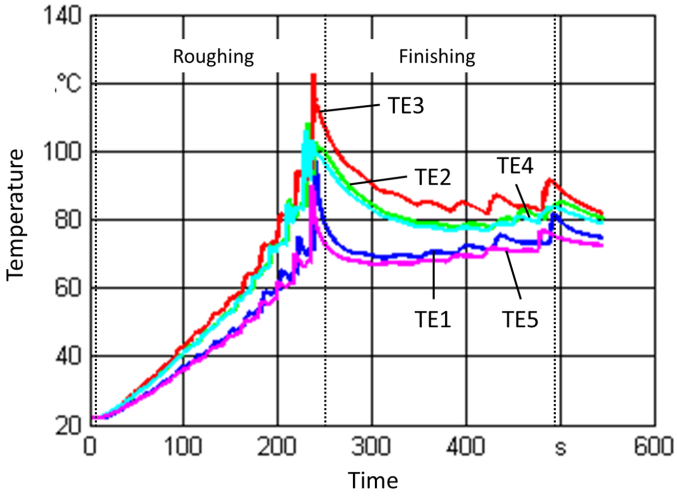

(b) Temperature in simulation

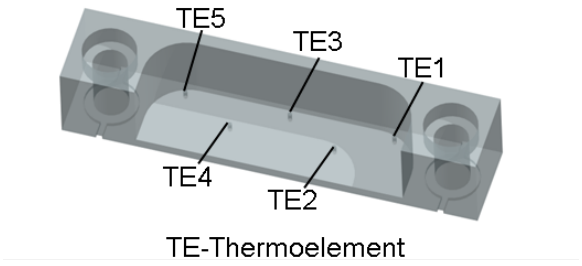

(c) Measuring points

FIGURE 5.2. Temperature over time on measuring points

REFERENCES

[1] J. W. Barrett and C. M. Elliott. A finite-element method for solving elliptic equations with Neumann data on a curved boundary using unfitted meshes. *IMA Journal of Numerical Analysis*, 4(3):309–325, 1984.

[2] J. W. Barrett and C. M. Elliott. Finite-element approximation of elliptic equations with a Neumann or Robin condition on a curved boundary. *IMA journal of numerical analysis*, 8(3):321–342, 1988.
[3] J. W. Barrett, H. Garcke, and R. Nürnberg. Finite-Element Approximation of One-Sided Stefan Problems with Anisotropic, Approximately Crystalline, Gibbs-Thomson Law. *arXiv preprint arXiv:1201.1802*, 2012.
[4] M. O. Benouamer and D. Michelucci. Bridging the gap between CSG and Brep via a triple ray representation. In *Proceedings of the fourth ACM symposium on Solid modeling and applications*, pages 68–79. ACM, 1997.
[5] D. Biermann, S. Grünert, and M. Steiner. A macroscopic approach towards the finite element simulation of tapping and thread milling of continuously reinforced extrusions. *Production Engineering*, 4(6):607–613, 2010.
[6] B Denkena and C Ammermann. Modular Numerical Control Model Including Realistic Motion Planning. In *International Conference on Product Lifecycle Management*, 2010.
[7] B. Denkena, P. Maaß, D. Niederwestberg, and J. Vehmeyer. Identification of the specific cutting force for complex cutting tools under varying cutting conditions. *Int. J. of Maschine Tools and Manufacture*, 2014. submitted.
[8] B. Denkena, A. Schmidt, J. Henjes, D. Niederwestberg, and C. Niebuhr. Modeling a thermomechanical NC-simulation. *Procedia CIRP*, 8:69–74, 2013.
[9] H. Muller, T. Surmann, M. Stautner, F. Albersmann, and K. Weinert. Online sculpting and visualization of multi-dexel volumes. In *Proceedings of the eighth ACM symposium on solid modeling and applications*, pages 258–261. ACM, 2003.
[10] R Pabst, J Fleischer, and J Michna. Modelling of the heat input for face-milling processes. *CIRP Annals-Manufacturing Technology*, 59(1):121–124, 2010.
[11] A. Schmidt and K.G. Siebert. *Design of Adaptive Finite Element Software: The Finite Element Toolbox ALBERTA*. Springer Heidelberg, 2005.
[12] E. Ungemach, A. Zabel, T. Surmann, R. Joliet, and A. Schröder. Simulation of the Temperature Distribution in NC-Milled Workpieces. *Advanced Materials Research*, 223:222–230, 2011.
[13] B. Denkena V. Boess, J. Brüning. *Concurrent Engineering Approaches for Sustainable Product Development in multi-Disciplinary Environment*. Springer London, 2013.
[14] D. Niederwestberg B. Denkena V. Böß, C. Ammermann. Contact Zone Analysis Based on Multidexel Workpiece Model and Detailed Tool Geometry. Procedia CIRP 4, 2012. published.
[15] T. Van Hook. Real-time shaded NC milling display. In *ACM SIGGRAPH Computer Graphics*, volume 20, pages 15–20. ACM, 1986.

The Center for Industrial Mathematics, University of Bremen, 28359 Bremen
E-mail address: niebuhr@math.uni-bremen.de

Institute of Production Engineering and Machine-Tools, Leibniz University of Hannover, 30823 Garbsen
E-mail address: niederwestberg@ifw.uni-hannover.de

The Center for Industrial Mathematics, University of Bremen, 28359 Bremen
E-mail address: schmidt@math.uni-bremen.de